



### **Science Arts & Métiers (SAM)**

is an open access repository that collects the work of Arts et Métiers Institute of Technology researchers and makes it freely available over the web where possible.

This is an author-deposited version published in: <https://sam.ensam.eu>  
Handle ID: <http://hdl.handle.net/10985/10925>

#### **To cite this version :**

Lamice DENGUIR, José OUTEIRO, Guillaume FROMENTIN, Vincent VIGNAL, Rémy BESNARD  
- Orthogonal cutting simulation of OFHC copper using a new constitutive model considering the state of stress and the microstructure effects - In: 7th CIRP HPC 2016, Allemagne, 2016-06-01 - Procedia CIRP - 2016

Any correspondence concerning this service should be sent to the repository

Administrator : [archiveouverte@ensam.eu](mailto:archiveouverte@ensam.eu)



# Orthogonal cutting simulation of OFHC copper using a new constitutive model considering the state of stress and the microstructure effects

L.A. Denguir<sup>a,b,\*</sup>, J.C. Outeiro<sup>a</sup>, G. Fromentin<sup>a</sup>, V. Vignal<sup>b,d</sup>, R. Besnard<sup>c,d</sup>

<sup>a</sup>LaBoMaP, Arts et Metiers ParisTech 71250 Cluny, FRANCE

<sup>b</sup>ICB UMR 6303 CNRS, Université de Bourgogne-Franche Comté, BP 47870, 21078 Dijon, FRANCE

<sup>c</sup>CEA Valduc, 21120 Is sur Tille, FRANCE

<sup>d</sup>LIMPE (Interaction Matériau-Procédé-Environnement), LRC DAM-VA-11-02, Dijon, FRANCE

\* Corresponding author. Tel.: +33-03-85-59-53-88; fax: +33-03-85-59-53-88. E-mail address: Lamice.DENGUIR@ensam.eu

---

## Abstract

This work aims to develop an orthogonal cutting model for surface integrity prediction, which incorporates a new constitutive model of Oxygen Free High Conductivity (OFHC) copper. It accounts for the effects of the state of stress on the flow stress evolution up to fracture. Moreover, since surface integrity parameters are sensitive to the microstructure of the work material, this constitutive model highlights also the recrystallization effects on the flow stress. Orthogonal cutting model is validated using experimental designed cutting tests. More accurate predictions were obtained using this new constitutive model comparing to the classical Johnson-Cook model.

(<http://creativecommons.org/licenses/by-nc-nd/4.0/>).

Peer-review under responsibility of the International Scientific Committee of 7th HPC 2016 in the person of the Conference Chair Prof. Matthias Putz

*Keywords:* Constitutive model; OFHC copper; Cutting; Finite element method (FEM); Modelling;

---

## 1. Introduction

Efforts on numerical modeling and simulation of metal cutting operations continue to increase due to the growing need for predicting the machining performance. However, the effectiveness of the numerical models to predict the machining performance depends on how accurately these models can represent the actual metal cutting process [1]. Several factors will influence accuracy of such models, including the incorrect description of the work material behavior in metal cutting. In the case of surface integrity, they are very sensitive to the energy required for separating the material from the workpiece to form the chip (energy of plastic deformation and fracture) [2]. Therefore, an improper modeling of the flow stress and fracture in metal cutting simulations leads to a high dispersion among the simulated results. Within the CIRP Working Group on “Surface Integrity and Functional Performance of Components”, a benchmark study was

conducted to evaluate the effectiveness of the current numerical predictive models for machining performance, including surface integrity [1, 2]. The predicted results clearly show a high dispersion among them, being this dispersion higher for the surface integrity.

The objective of this work is to propose a consolidated physical modelling approach for predicting surface integrity induced by machining OFHC copper. This approach incorporates a new constitutive model that accounts for the effects of the state of stress and microstructure on the flow stress. Moreover, it incorporates a physical-based model for microstructure prediction induced by machining.

## 2. Consolidated physical modeling (CPM)

This study concerns annealed (2h at 450°C) OFHC copper, a monophasic material with an average grain size ( $d_0$ ) of 62  $\mu\text{m}$ , and an initial dislocation density ( $\rho_0$ ) of  $4.2 \times 10^{13} \text{m}^{-2}$ .

## 2.1. Material constitutive model

The proposed material constitutive model takes into consideration the most relevant phenomena influencing the material behavior. It was inspired from phenomenological models (including the Johnson-Cook constitutive model [3]) taking into account the strain hardening, the strain rate, the temperature [3], the microstructural transformation [4], and the state of stress effects [5]. The flow stress ( $\bar{\sigma}$ ) is expressed by the following equation (Eq. 1).

$$\bar{\sigma} = \underbrace{\left[ A + B\varepsilon^n \right]}_{\text{Strain hardening effect}} \times \underbrace{\left[ 1 + C \ln\left(\frac{\dot{\varepsilon}}{\dot{\varepsilon}_0}\right) \right]}_{\text{Strain-rate (viscosity) effect}} \times \underbrace{\left[ 1 - \left( \frac{T - T_{room}}{T_m - T_{room}} \right)^m \right]}_{\text{Thermal softening effect}} \times \underbrace{H(\varepsilon, \dot{\varepsilon}, T)}_{\text{Microstructural transformation effect}} \times \underbrace{\left[ 1 - c_\eta (\eta - \eta_0) \right]}_{\text{State of stress effect}} \quad (1)$$

Its particularity comes from the proposed  $H(\varepsilon, \dot{\varepsilon}, T)$  function (Eq. 2) introducing the microstructural effect, especially dynamic recrystallization. This function couples the effect of strain, strain-rate and temperature as three of them influence this phenomenon. Indeed, it is activated by the ( $u$ ) function (Eq. 3) only in case the strain exceeds the recrystallization strain threshold ( $\varepsilon_r$ ), calculated using the equation proposed by Liu et al. [6] for OFHC copper (Eq. 6).

$$H(\varepsilon, \dot{\varepsilon}, T) = \frac{1}{1 - \bar{H}(\varepsilon, \dot{\varepsilon}) \times u(\varepsilon, \dot{\varepsilon}, T)} \quad (2)$$

$$u(\varepsilon, \dot{\varepsilon}, T) = \begin{cases} 0 & \text{when } \varepsilon < \varepsilon_r \\ 1 & \text{when } \varepsilon \geq \varepsilon_r \end{cases} \quad (3)$$

$$\bar{H}(\varepsilon, \dot{\varepsilon}) = \hat{H}_1(\varepsilon) - \hat{H}_2(\varepsilon) \times \exp(\dot{\varepsilon}) \quad (4)$$

$$\hat{H}_i(\varepsilon) = \frac{h_0}{\varepsilon} + h_i \quad \text{with } i = 1 \dots 2 \quad (5)$$

$$\varepsilon_r(\varepsilon, T) = e_0 \left[ \log_{10}(\varepsilon) + e_1 \times \exp\left(\frac{e_2}{T - T_{ref}}\right) \right] \quad (6)$$

Concerning to the state of stress effect, only the triaxiality parameter ( $\eta$ ) (the ratio between the hydrostatic stress and von Mises equivalent stress) is considered. The proposed constitutive model coefficients of Eq.1 ( $A$ ,  $B$ ,  $C$ ,  $n$ ,  $m$ ,  $h_i$  ( $i=0 \dots 2$ ) and ( $c_\eta$ ) are identified basing on material characterization tests described as follows. Three kinds of mechanical tests were performed. To identify the constants corresponding to the strain hardening effect, uniaxial compression tests were led on cylindrical specimens with a Gleeble machine at low strain rates ( $0.1 \text{ s}^{-1}$ ,  $1 \text{ s}^{-1}$  and  $10 \text{ s}^{-1}$ ) at  $20^\circ\text{C}$ ,  $200^\circ\text{C}$ ,  $400^\circ\text{C}$  and  $600^\circ\text{C}$ . For the constants corresponding to the strain-rate effect, split Hopkinson pressure bars tests were led on cylindrical specimens at high strain-rates ( $700 \text{ s}^{-1}$ ,  $1600 \text{ s}^{-1}$  and  $2000 \text{ s}^{-1}$ ) at  $27^\circ\text{C}$ ,  $500^\circ\text{C}$  and  $650^\circ\text{C}$ . Several temperature levels were used to identify the thermal softening coefficients, as well as those coefficients related to the microstructural transformation effect. As far as the state of stress effect is concerned, uniaxial compressive (cylindrical specimens [5]) and tensile tests (flat grooved specimens) were performed to evaluate the influence of different stress triaxiality values on the flow stress. Using a

hybrid experimental-numerical procedure described in [5], the ( $c_\eta$ ) was identified. All the coefficients are in Table 1.

Table 1. List of the constitutive model constants.

Constant	Value	Constant	Value
$A$ (MPa)	125	$e_0$ [6]	0.243
$B$ (MPa)	316	$e_1$ [6]	9.5
$n$	0.44	$e_2$ [6]	$-1.863 \times 10^{-8}$
$C$	0.014	$e_3$ [6]	-2.69
$\dot{\varepsilon}_0$ ( $\text{s}^{-1}$ )	0.1	$h_0$	1.93
$m$	0.7	$h_1$	0.82
$T_{room}$ ( $^\circ\text{C}$ )	20	$h_2$	0.48
$T_m$ ( $^\circ\text{C}$ )	1085	$c_\eta$	0.1
		$\eta_0$	-0.33

## 2.2. Microstructure prediction model

The microstructure parameters are predicted using the dislocation density based model proposed by Estrin and Kim [7]. It aims to calculate the total dislocation density ( $\rho_{tot}$ ) evolution and grain size ( $d$ ). It makes a distinction between the two kinds of dislocations densities: those in the walls ( $\rho_w$ ) and those in the cells interiors ( $\rho_c$ ). Knowing the volume fraction of the walls ( $f$ ) given by Eq. 7, the total dislocation density can be calculated using Eq. 8:

$$f = f_\infty + (f_0 - f_\infty) \times \exp\left(-\frac{\gamma_r}{\bar{\gamma}_r}\right) \quad (7)$$

$$\rho_{tot} = f \times \rho_w + (1 - f) \times \rho_c \quad (8)$$

$$\frac{d\rho_w}{d\gamma_r} = \frac{6\beta^*(1-f)^{2/3}}{bdf} + \frac{\sqrt{3}\beta^*(1-f)\sqrt{\rho_w}}{fb} - k_0 \left(\frac{\dot{\gamma}_r}{\bar{\gamma}_r}\right)^n \rho_w \quad (9)$$

$$\frac{d\rho_c}{d\gamma_r} = \alpha^* \frac{1}{\sqrt{3}} \frac{\sqrt{\rho_w}}{b} - \beta^* \frac{6}{bd(1-f)^{1/3}} - k_0 \left(\frac{\dot{\gamma}_r}{\bar{\gamma}_r}\right)^n \rho_c \quad (10)$$

where ( $f_0$ ) and ( $f_\infty$ ) are initial and saturation values of ( $f$ ), equal to 0.077 and 0.25 respectively. Moreover, ( $\bar{\gamma}_r$ ) is the variation of ( $f$ ) with the resolved shear strain ( $\gamma_r$ ) which is equal to  $3.2 \text{ s}^{-1}$ . Dislocation densities in the cells and in the walls are governed by Eq. 9 and Eq. 10 basing on the reactions that are susceptible to occur due to density dislocation nucleation, annihilation and interaction. Their description and the values of the used parameters for OFHC copper are detailed in the reference [7].

In order to calculate the grain refinement on the machined surface, the average grain size ( $d$ ) is assumed to evolve linearly with the inverse of the square root of the total dislocation density ( $\rho_{tot}$ ) [7], as shows Eq. 11. The value of the parameter ( $K$ ) is identified knowing initial grain size ( $d_0$ ) of the bulk material and its initial dislocation density ( $\rho_0$ ).

$$d = \frac{K}{\sqrt{\rho_{tot}}} \quad (11)$$

As the micro-hardness Vickers ( $HV$ ) is correlated to grain size, it is possible to predict it using the equation (Eq. 12) proposed by Rotella and Umbrello [8], with ( $c_{HV1}$ ) and ( $c_{HV2}$ ) two constants equal to 77 and  $18 \mu\text{m}^{0.5}$  respectively.

$$HV = c_{HV1} + \frac{c_{HV2}}{\sqrt{d}} \quad (12)$$

### 3. Orthogonal cutting model and validation

In order to evaluate the proposed *CPM* approach to predict surface integrity parameters, an orthogonal cutting model was developed and validated using experimental cutting tests data. The tool is made of carbide with a rake angle ( $\gamma$ ) of 30°, a flank angle ( $\alpha$ ) of 10°, and a cutting edge radius of ( $r_n$ ) of 10±2 μm. The cutting speed ( $v_c$ ) was 90 m/min, the uncut chip thickness ( $h$ ) was 0.2 mm and the width of cut was 4 mm.

#### 3.1. Orthogonal cutting model

A numerical model based on the Arbitrary Lagrangian–Eulerian (*ALE*) formulation was developed and applied to simulate the surface integrity induced by orthogonal cutting of OFHC copper. A coupled temperature displacement analysis was performed using the *FEA* software ABAQUS/Explicit. To model the flow stress behavior and the microstructure evolution of OFHC copper, a user subroutine VUMAT was developed to integrate the *CPM* approach described in §2 in the numerical simulations. The elastic and thermal properties of the work material were obtained from experimental tests on the same work material as those used in the machining tests. The tool was modelled as elastic and its thermal and elastic properties were obtained from literature [9]. Concerning to the tool-chip and the tool-workpiece contacts, they were modelled using the Zorev's model [10], being the friction coefficient ( $\mu$ ) given by (Eq.13). Its description and parameters are reported by Outeiro *et al.* [10].

$$\mu = c_1 + \frac{c_2}{1 + \left[ \frac{v_s - c_3}{c_4} \right]} \quad (13)$$

For residual stresses prediction, the model has been transferred to ABAQUS/Standard which is based on the implicit time integration, suitable to reach the stress equilibrium in a reduced time.

#### 3.2. Experimental cutting tests

The orthogonal cutting tests using a planing configuration were performed on a CNC milling machine. The experimental setup used for force measurements is described in [10]. After these machining tests, Vickers micro-hardness was measured on each specimen using micro-hardness tester, applying a charge of 25 g. Residual stresses analysis were conducted on the machined specimen by X-ray diffraction technique and using the  $\sin^2\psi$  method. According to this method, the residual stresses were calculated from strain distribution ( $\varepsilon_{\varphi\psi/hkl}$ ) derived from the measured interreticular plane spacing and knowing the elastic radiocrystallographic elastic constants, ( $S_{1(hkl)}$ ) and ( $\frac{1}{2}S_{2(hkl)}$ ), which are equal to  $-3.13 \times 10^6 \text{ MPa}^{-1}$  and  $11.7 \times 10^6 \text{ MPa}$  for OFHC copper, respectively. An X-ray *Mn-K $\alpha$*  radiation was used to determine the elastic strains in the (311) planes (149.09°

Bragg angle). Residual stresses were analyzed in the machined surface and subsurface in the cutting ( $\sigma_{//}$ ) and transversal ( $\sigma_{\perp}$ ) directions. To evaluate the residual stresses at subsurface, successive layers of material were removed by electro-polishing, to avoid the reintroduction of residual stress.

### 4. Results and discussion

Comparing the prediction results using both Johnson-Cook (*J-C*) (Eq. 1 with the strain, strain-rate and thermal effects only) and the new model (Eq. 1) to the experimental results has revealed the limits of each one. As far as the cutting force ( $F_c$ ) is concerned, both J-C and the new model under estimate this force (660±20 N for the J-C model and 750±50 N for the new model) when compared to the experimental force value (927±113 N). However, the force predicted by the new model is closer and within the error of the measured force. Concerning to the chip compression ratio (*CCR*), predictions are in good agreement with the experimental values (measured *CCR* value is 2.25±0.15, while the simulated ones are 2.62 for the new model and 2.08 for the J-C model).

As far as surface integrity is concerned, residual stresses and grain size distributions at surface and subsurface were evaluated. Micrographic analysis (Fig. 1a) has revealed an average grain size ( $d$ ) at the machined surface of 6±5 μm and a refined layer thickness of about 100±10 μm (Fig. 1b).

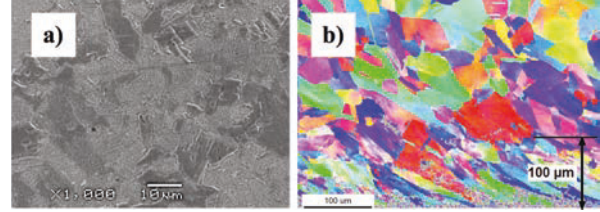


Fig. 1. Micrography of (a) the machined surface by SEM (b) the specimen cross-section by EBSD.

Results issued from both models (Fig. 2) are in good agreement with the experimental concerning the grain size at the top surface (4 μm for the J-C model and 2 μm for the new model). Nevertheless, a slight improvement is seen in the affected layer thickness prediction when the new model is used (64 μm for the J-C model and 97 μm for the new one). It should be pointed out that due to the effect of the etchant used for grains revelation, the experimentally measured grain size value should correspond to a depth of few microns under the machined surface, which seems in accordance with simulations.

The accuracy of the micro-hardness model was also tested. According to the results (Fig. 3), it fits well the hardness trend while simulating with both J-C and the new models.

Nevertheless, the impact of the material model modification is more noticeable in the residual stresses prediction. In fact, Fig. 4 and Fig. 5 show that the proposed model gives better prediction of the residual stresses than the J-C model, although a gap is still prevailing between the

numerical simulations and the experimental measurements, in particular for depths higher than 300  $\mu\text{m}$ .

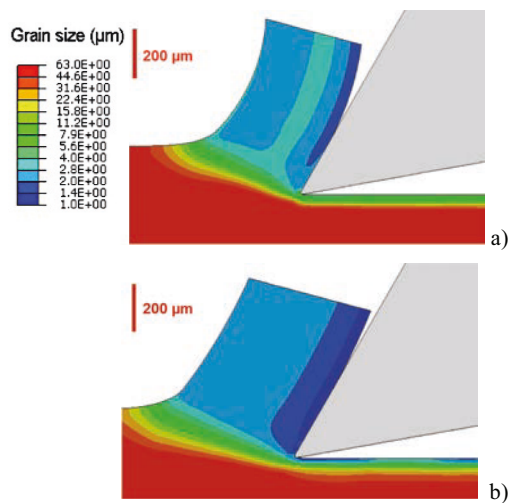


Fig. 2. Simulated grain size distribution using (a) J-C (b) the new model

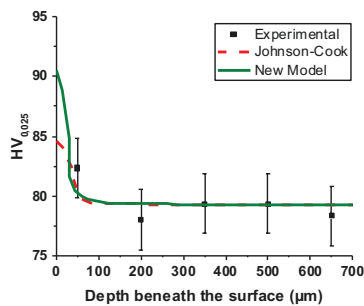


Fig. 3. Experimental and predicted Vickers micro hardness ( $HV_{0.025}$ )

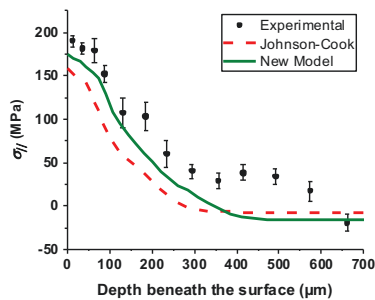


Fig. 4. Experimental and predicted residual stresses in cutting direction ( $\sigma_y$ ).

## 5. Conclusion

In view of the results, an improvement has been established in the prediction of the surface integrity using the new constitutive model considering the state of stress and the microstructure effects comparing to the traditional Johnson-Cook model.

In fact, an enhancement is seen in simulations results concerning cutting forces, chip compression ratio, average grain size, micro-hardness and residual stresses predictions. Nevertheless, more enhancements should be done on this proposed model in order to obtain better predictions.

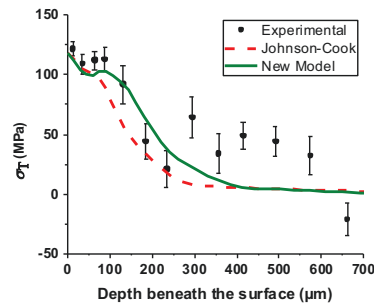


Fig. 5. Experimental and predicted residual stresses in transversal direction ( $\sigma_x$ ).

## Acknowledgements

The authors would like to acknowledge CEA Valduc the financial support and thank Mr. S. Flouriot, Dr. A.C. Batista, Dr. S. Campocasso and Dr. B. Marcon for the valuable help in material characterization and tests monitoring.

## References

- [1] Jawahir, I. S., Brinksmeier, E., M'Saoubi, R., Aspinwall, D. K., Outeiro, J. C., Meyer, D., Umbrello, D., Jayal, A.D., 2011, Surface integrity in material removal processes: Recent advances, *CIRP Annals*, 60/2:603–626.
- [2] Outeiro, J. C., Umbrello, D., M'Saoubi, R., Jawahir, I. S., 2015, Evaluation of Present Numerical Models for Predicting Metal Cutting Performance And Residual Stresses, *Machining Science and Technology*, 19/2:183–216.
- [3] Johnson, G. R., Cook, W. H., 1985, Fracture characteristics of three metals subjected to various strains, strain rates, temperatures and pressures, *Engineering Fracture Mechanics*, 21/1:31–48.
- [4] Andrade, U.R., Meyers, M.A., Chokshi, A.H., 1994, Constitutive description of work and shock-hardened copper, *Scripta Metallurgica Materialia*, 30/7 :933-938.
- [5] Bai, Y., Wierzbicki, T., 2008, A new model of metal plasticity and fracture with pressure and Lode dependence , *International Journal of Plasticity* 24:1071-1096.
- [6] Liu, R., Salahshoor, M., Melkote., S.N, Marusich, T., 2015, A unified material model including dislocation drag and its application to simulation of orthogonal cutting of OFHC Copper, *Journal of Materials Processing Technology*, 216 :328-338.
- [7] Estrin, Y., Kim, S.K., 2007, Modelling microstructure evolution towards ultrafine crystallinity produced by severe plastic deformation, *Journal of Materials Science*, 42 :9092-9096.
- [8] Rotella, G., Dillon, O.W.Jr., Umbrello, D., Settineri, L., Jawahir, I.S., 2013, Finite element modeling of microstructural changes in turning of AA7075-T651 alloy, *Journal of Manufacturing Processes* 15 :87-97.
- [9] Outeiro, J. C., Dias, A. M., Jawahir, I. S., 2006, On the effects of residual stresses induced by coated and uncoated cutting tools with finite edge radii in turning operations, *CIRP Annals*, 55/1:111–116.
- [10] Outeiro, J. C., Campocasso, S., Denguir, L.A., Fromentin, G., Vignal, V., Poulachon, G., 2015, Experimental and numerical assessment of subsurface plastic deformation induced by OFHC copper machining, *CIRP Annals*, 64/1 :53-56.